Electron paramagnetic resonance of non-Kramers ion in a fluorozirconate glass



1991 J. Phys.: Condens. Matter 3 1889

(http://iopscience.iop.org/0953-8984/3/12/019)

J. Phys.: Condens. Matter 3 (1991) 1889–1900. Printed in the UK

# Electron paramagnetic resonance of non-Kramers ions in a fluorozirconate glass

E A Harris and D Furniss
*Department of Physics, University of Sheffield, PO Box 597, Sheffield S10 2UN, UK*

Received 24 August 1990

**Abstract.** Electron paramagnetic resonance of trivalent thulium and terbium ions in a multicomponent fluorozirconate glass is reported. A theoretical reconstruction is described that accounts well for the observed spectra. The signals arise from ions having doublet ground states with a continuous distribution of zero-field splittings from zero upwards. Spin Hamiltonian parameters were measured as: $g_\parallel = 13.7 \pm 0.3$, $A_\parallel/g_\parallel\mu_B = 24.5 \pm 1.0$ mT for $Tm^{3+}$ and $g_\parallel = 17.5 \pm 0.2$, $A_\parallel/g_\parallel\mu_B = 24.9 \pm 0.4$ mT for $Tb^{3+}$. These correspond to ions in essentially $|\pm 6\rangle$ states. Probable sites are discussed and the spectra are shown to be consistent with 8-coordinated $Tm^{3+}$ in square antiprism sites and 9-coordinated $Tb^{3+}$ in tricapped trigonal prism sites, although other types of site probably also occur.

## 1. Introduction

In the last few years many papers have been published on the properties of heavy-metal fluoride glasses, particularly those based on $ZrF_4$. They are of special interest because of their high transparency from 250 nm in the ultraviolet through the visible to 7 $\mu$m in the infrared. These glasses have been developed for use in ultra-low-loss optical fibres at 2.5 $\mu$m and are easily doped with rare-earth ions with possible applications as solid-state lasers and for up-conversion of infrared radiation into visible fluorescence [1]. Although most interest has centred on the optical properties, electron paramagnetic resonance (EPR) measurements can provide valuable information about the local site symmetries and the nature of the ground states of rare-earth and other paramagnetic ions in these glasses. The EPR technique has had great success in the study of crystalline solids, where very detailed information about the local environment of a paramagnetic ion can be obtained from the dependence of the EPR spectrum on applied field direction. In glasses the technique has also been widely used [2], but the analysis is complicated because the geometries vary from one ionic site to another and the measured EPR represents an average over all possible orientations. Most work has been done on ions of the iron group; of the rare-earth group only the S-state ions $Gd^{3+}$ and $Eu^{2+}$ have been extensively studied. For the other rare-earth ions there is generally a large orbital contribution to the ground state, which makes it very sensitive to variations in the local electric field, leading to strong anisotropy in the $g$-tensors, severe inhomogeneous broadening of the resonance and short spin–lattice relaxation times. These effects mean that usually the EPR can only be observed at liquid-helium temperatures, and even then the resonances are broad and consequently hard to measure and interpret.

0953-8984/91/121889 + 12 $03.50 

**Table 1.** Some properties of trivalent terbium and thulium.

| | $Tb^{3+}$ | $Tm^{3+}$ |
|---|---|---|
| Configuration | $4f^8$ | $4f^{12}$ |
| Ground state | $^7F_6$ | $^3H_6$ |
| Landé factor, $g_J$ | 3/2 | 7/6 |
| Nucleus | $^{159}Tb$ | $^{169}Tm$ |
| Nuclear spin, $I$ | 3/2 | 7/2 |

An earlier paper [3] has described EPR measurements on $Tb^{3+}$ in a fluorozirconate glass, from which it was clear that the ground state is a closely spaced doublet corresponding to the maximum possible $M_J$ values: $|M_J\rangle = |\pm J\rangle = |\pm 6\rangle$. Similar measurements on $Tm^{3+}$ EPR reported here show that this ion also has a doublet ground state corresponding to $|M_J\rangle = |\pm J\rangle = |\pm 6\rangle$. Although such a ground state could occur 'accidentally' it is surprising that the accident should happen twice.

Some of the properties of trivalent terbium and thulium are shown in table 1. Both are non-Kramers ions, i.e. ions with an even number of electrons and an integral electronic angular momentum $J$. In a solid the ligand-field interaction can completely remove the electronic degeneracy of a non-Kramers ion ground state to give a set of $2J + 1$ singlets. The energy separation of the lowest levels is usually too large to be spanned by the available EPR microwave quantum and no EPR is observed. Sometimes some degeneracy may remain, either accidentally or when the ion is in a site of high symmetry, and EPR is possible, but even then it is very sensitive to variations in site geometry resulting in strong inhomogeneous line broadening. For these reasons, even in crystalline hosts, measurements on $Tb^{3+}$, $Tm^{3+}$ and the other non-Kramers lanthanide ions have been much less frequently reported than those on Kramers ions. In a glass the inhomogeneous broadening can be less of a problem because the resonance is already spread out over a large field range by the orientational distribution, and the inhomogeneous broadening merely redistributes the EPR intensity within this range.

In the following section we derive an expression for the EPR lineshape expected to arise in this way for ions with a non-Kramers doublet ground state. Although the derivation is based on that presented previously [3], it differs in detail in the assumed direction of the microwave magnetic field. The EPR spectra for $Tb^{3+}$ and $Tm^{3+}$ are then compared with this theoretical prediction and shown to be consistent with ground states characterized by $|M_J\rangle = |\pm 6\rangle$. Finally the implications of these results will be discussed in relation to the probable rare-earth-ion site geometries.

## 2. Theory of the electron paramagnetic resonance lineshape

The ground state is treated in terms of an effective spin $s = \frac{1}{2}$ with the usual spin Hamiltonian for a non-Kramers doublet [4]:

$$\mathcal{H} = g_\parallel \mu_B B_z s_z + \delta s_x + A_\parallel I_z s_z \tag{1}$$

The term $\delta s_x$ gives rise to a zero-field energy splitting and also mixes the two states, removes the time conjugacy and allows a transition probability between them when the

microwave field $\boldsymbol{b}$ has a component parallel to the $z$ direction. A term $\delta' s_y$ could also be included, but such a term can be eliminated by a simple coordinate rotation or a different choice of phase of the states and so produces no extra physical effect. For the terbium ions ($I = \frac{3}{2}$) there could also be an electric quadruple hyperfine interaction, but it is small and will not be discussed here.

It is assumed that each of the magnetic ions is described by equation (1) but that the axes of quantization $z$ are in random directions $(\theta, \varphi)$. It is also assumed that there are only small variations in local site geometry from ion to ion, so the parameters $g_\parallel$ and $A_\parallel$ are taken as constants. The parameter $\delta$ is much more sensitive to these variations and is allowed a range of values from zero upwards, given by a distribution function $P(\delta)$. The direction of the applied magnetic field $\boldsymbol{B}$ defines the polar axis ($\theta = 0$) of the spherical polar coordinate system. The microwave field $\boldsymbol{b}$ is assumed to be normal to $\boldsymbol{B}$, corresponding to the experimental situation in the EPR cavity, and is taken to lie along the azimuthal axis ($\theta = \pi/2$, $\varphi = 0$). In this respect the following analysis differs from that presented previously [3] where the direction of $\boldsymbol{b}$ was assumed random.

The energy levels obtained by diagonalizing equation (1) are

$$W_{1,2} = \pm[\delta^2 + (g_\parallel \mu_B B_z + A_\parallel m)^2]^{1/2} \tag{2}$$

where $B_z = B\cos\theta$ and $m$ is the eigenvalue of $I_z$. As there are no off-diagonal matrix elements involving $m$, it is a good quantum number, which can be used to label the states. Since $g_\perp = 0$, magnetic dipole transitions can be induced only by a microwave field component $b_z$ through a perturbation

$$\mathcal{H}' = g_\parallel \mu_B s_z b_z. \tag{3}$$

Thus they obey a selection rule $\Delta M_s = 0$, $\Delta m = 0$, and the resonance condition for a microwave frequency $\nu$ is

$$h\nu = [\delta^2 + (g_\parallel \mu_B B_z + A_\parallel m)^2]^{1/2}. \tag{4}$$

The eigenstates corresponding to (2) are

$$\psi_{1,2} = \cos\alpha|\pm\tfrac{1}{2}, m\rangle \pm \sin\alpha|\mp\tfrac{1}{2}, m\rangle \tag{5}$$

where

$$\sin(2\alpha) = \delta[\delta^2 + (g_\parallel \mu_B B_z + A_\parallel m)^2]^{-1/2} = \delta/h\nu. \tag{6}$$

The transition probability is proportional to

$$T = |\langle\psi_1|\mathcal{H}'|\psi_2\rangle|^2 = [\tfrac{1}{2} g_\parallel \mu_B b_z \sin(2\alpha)]^2 \tag{7}$$

where $b_z = b\sin\theta\cos\varphi$. As all values of $\varphi$ are equally probable and $\varphi$ does not affect the resonance field, equation (7) is averaged over all $\varphi$ to give a mean transition probability

$$T = [g_\parallel \mu_B b \sin\theta \sin(2\alpha)]^2/8. \tag{8}$$

Electric dipole transitions can also be important for ions in sites that lack reflection symmetry [4], but we neglect them here. Experimentally the samples were positioned in the cavity in a region where the microwave electric field was close to zero and the measured lineshapes provide no evidence for such a contribution.

The total EPR signal observed in an applied field $\boldsymbol{B}$ can contain contributions from centres oriented such that their field components $B_z$ is in the range from zero to $|\boldsymbol{B}|$.

There will be separate contributions from each $m$ value. Thus the EPR signal strength in the field range $B$ to $B + \mathrm{d}B$ is

$$I(B)\,\mathrm{d}B = \mathrm{d}B \sum_m \int_0^B N(\theta)(d\theta/\mathrm{d}B)U(B_z)\,\mathrm{d}B_z. \tag{9}$$

Here $N(\theta)\,\mathrm{d}\theta$ is the relative number of ions oriented in the angular range $\mathrm{d}\theta$, and with a random distribution is given by

$$N(\theta)\,\mathrm{d}\theta = \sin\theta\,\mathrm{d}\theta = (B_z/B^2)\,\mathrm{d}B. \tag{10}$$

The factor $U(B_z)\,\mathrm{d}B_z$ is the signal strength associated with field components in the range $B_z$ to $B_z + \mathrm{d}B_z$. This will arise from just those ions whose $\delta$ values satisfy equation (4) and will thus depend on their probability density $P(\delta)\,\mathrm{d}\delta$, i.e.

$$U(B_z)\,\mathrm{d}B_z = TP(\delta)|\mathrm{d}\delta/\mathrm{d}B_z|\,\mathrm{d}B_z. \tag{11}$$

Writing $x = p + qB_z$, where $p = A_\parallel m/h\nu$ and $q = g_\parallel \mu_B/h\nu$, and defining $C = (h\nu/g_\parallel\mu_B B)^2$, equation (9) becomes

$$I(B)\,\mathrm{d}B = \mathrm{d}B g_\parallel \mu_B h\nu (b^2/8B^2) \sum_m \int_p^{p+qB} |f(x)|\,\mathrm{d}x \tag{12}$$

where

$$\begin{aligned} &\text{if } |x| \leqslant 1 \qquad f(x) = x(x-p)[1 - C(x-p)^2](1-x^2)^{1/2}P(\delta) \\ &\text{if } |x| \geqslant 1 \qquad f(x) = 0. \end{aligned} \tag{12a}$$

If $P(\delta)$ is a simple function, then the integral can be evaluated without difficulty. We have done this for two cases.

(i) If $P(\delta)$ is constant ($=1$):

$$\begin{aligned} F(x) = \int f(x)\,\mathrm{d}x &= (2 - C - 6Cp^2)[\sin^{-1}x + x(2x^2-1)(1-x^2)^{1/2}]/16 \\ &+ (1-x^2)^{3/2}[cx^3/6 - Cp(3x^2+2)/5 + p(1-Cp^2)/3]. \end{aligned} \tag{13a}$$

(ii) If $P(\delta)$ is proportional to $\delta (= (1-x^2)^{1/2})$:

$$\begin{aligned} F(x) = \int f(x)\,\mathrm{d}x &= C(x^7/7 - x^5/5) + 3pC(x^4/4 - x^6/6) \\ &+ (1 - 3Cp^2)(x^3/3 - x^5/5) + (Cp^3 - p)(x^2/2 - x^4/4). \end{aligned} \tag{13b}$$

Equations (13*a*, *b*) are valid only in the range $-1 < x < 1$. For $x < -1$, $F(x) = F(-1)$; and for $x > 1$, $F(x) = F(1)$.

By substituting into equation (13) and applying the limits, the following result is obtained for the calculated EPR lineshape:

$$I(B)\,\mathrm{d}B = \mathrm{d}B g_\parallel \mu_B h\nu (b^2/8B^2) \sum_m G \tag{14}$$

where

$$\begin{aligned} &\text{for } A_\parallel m > 0 && G = F(p+qB) - F(p) \\ &\text{for } A_\parallel m < 0,\ A_\parallel m + g_\parallel \mu_B B > 0 && G = F(p+qB) + F(p) - 2F(0) \\ &\text{for } A_\parallel m + g_\parallel \mu_B B < 0 && G = F(p) - F(p+qB). \end{aligned} \tag{14a}$$

The expression (14) has been computed and digitally differentiated with respect to field

for comparison with experimentally observed EPR spectra. Some examples are shown in figures 1 and 3.

The main features predicted are associated with discontinuities in $|f(x)|$ at $x = 0$ and $x = \pm 1$. The $x = 0$ condition corresponds to $B_z = A_\parallel m/g_\parallel \mu_B$ and will affect the intensity for an applied field $B \geqslant A_\parallel m/g_\parallel \mu_B$. This condition is unusual for EPR in being independent of microwave frequency and provides a measurement of the ratio $A_\parallel/g_\parallel$. The $x = \pm 1$ conditions correspond to $g_\parallel \mu_B B_z = \pm h\nu - A_\parallel m$ and allow independent determination of $A_\parallel$ and $g_\parallel$. The $x = 0$ and $x = \pm 1$ features are associated with ions for which $\delta = h\nu$ and $\delta = 0$ respectively. The observation of features of both types indicates an appreciable number of ions over the whole range of $\delta$ values from zero up to the microwave quantum. The expression (14) for $I(B)$ differs from that given previously [3]. The earlier expression, which does not allow for the correct direction of the microwave field, may be obtained if $C$ in equations (13*a*, *b*) is replaced by zero.

### 3. *Results for thulium*

The EPR measurements on $Tm^{3+}$ were made using a frequency of 9.17 GHz on a Varian 4502 spectrometer fitted with a helium gas flow cryostat. The composition of the glass studied was (mol%) 51.9 $ZrF_4$, 19.7 $BaF_2$, 18.1 NaF, 3.2 $AlF_3$, 2.5 $PbF_2$, 4.6 $TmF_3$. More dilute samples were also prepared with 90% of the $TmF_3$ replaced by $LaF_3$, but the EPR signals in these were too weak to measure accurately. The strongest signals were seen at the lowest available temperatures, 4.5 K. At higher temperatures the signals rapidly broadened and weakened. A typical spectrum is shown in figure 1, where it is compared with theoretical reconstructions. The features at $g_\parallel \mu_B B = h\nu \pm \frac{1}{2}A_\parallel$ should appear as discontinuities in the curvature of this derivative spectrum, which are difficult to locate precisely. On a second-derivative curve they should appear as cusps. Accordingly the second derivative was calculated digitally from the experimental curve and values for the two parameters $A_\parallel$ and $g_\parallel$ determined from this:

$$g_\parallel = 13.7 \pm 0.3 \qquad A_\parallel/g_\parallel \mu_B = 24.5 \pm 1.0\ \text{mT}.$$

A second-derivative curve is shown in figure 2, where it is again compared with spectra

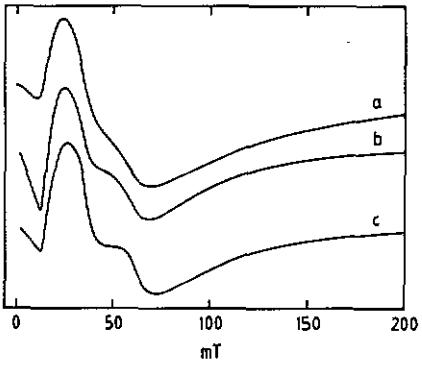


**Figure 1.** The EPR spectra of $Tm^{3+}$ at 9.17 GHz: (*a*) experimental; (*b*) theoretical reconstruction with $P(\delta) \propto \delta$; (*c*) theoretical reconstruction with $P(\delta) =$ constant.

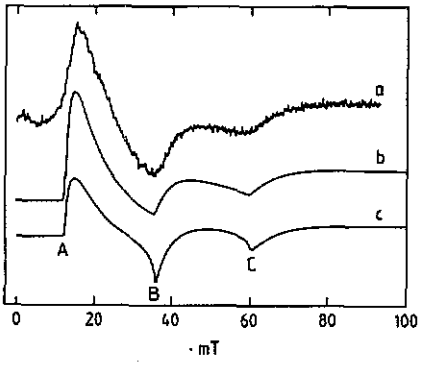


**Figure 2.** Second derivative of the $Tm^{3+}$ EPR spectra at 9.17 GHz: (*a*) experimental; (*b*) theoretical; reconstruction with $P(\delta) \propto \delta$; (*c*) theoretical reconstruction with $P(\delta) =$ constant.

reconstructed using the above parameters. Allowing for a small amount of line broadening, due to either lifetime or inhomogeneous effects, which will round off the predicted cusps, the agreement between experiment and theory is good, bearing in mind that there are only two adjustable parameters in the model. The positions of the main features are not affected by the form of $P(\delta)$. Comparing the experimental lineshape with the two reconstructions, it is difficult to choose either form as being appreciably better than the other. In view of this insensitivity of $I(B)$ to the form of $P(\delta)$, it did not seem worth while to reconstruct spectra with other forms of $P(\delta)$. The feature (A) at lowest field, given by $g_\parallel \mu_B B = \frac{1}{2}A_\parallel$, is associated with ions having $\delta \simeq h\nu$ and the other features (B, C), given by $g_\parallel \mu_B B = h\nu \pm \frac{1}{2}A_\parallel$, are associated with ions having $\delta$ approaching zero. It is thus clear that $\delta$ covers a range of values from zero to at least 0.3 $cm^{-1}$. In both reconstructions, features B and C appear more clearly than in the experimental curve. The only obvious modification to the model would be to allow $g_\parallel$ and $A_\parallel$ to take a range of values. If admixtures of states of different $J$ are negligible, the ratio $A_\parallel/g_\parallel$ should remain constant and equal to $A_J/g_J$, so the low-field feature A would not be shifted or appreciably broadened. The observed positions of B and C correspond to a $g_\parallel$ close to $12g_J = 14$, the maximum possible for this ion, so the main effect will be a broadening of features B and C coupled with a shift towards higher field. This probably accounts for the small differences between the experimental and reconstructed spectra. The signal-to-noise ratio does not justify attempts to distinguish between the effects of different forms of $P(\delta)$ and the effects of $g_\parallel$ variations. We believe the latter are relatively small and that the EPR is due to ions in states that are predominantly $|M_J\rangle = |\pm 6\rangle$.

## 4. Results for terbium

Some EPR spectra for $Tb^{3+}$ are compared with theoretical reconstructions in figures 3 and 4. The agreement is better than with the more primitive theory reported previously [3]. The reconstructions use parameters derived by measuring field positions of the cusps in the higher-field part of the second-derivative spectrum: $g_\parallel = 17.5 \pm 0.2$, $A_\parallel/g_\parallel\mu_B = 24.9 \pm 0.4$ mT. In the lower-field part of the spectrum the agreement is less good due, we believe, to the small nuclear quadrupole interaction, which produces features where energy levels cross [3].

A notable experimental feature is a sharp frequency dependence of the spectrum around zero field when the size of the microwave quantum is near to 0.314 $cm^{-1}$. This energy is interpreted as exactly matching the zero-field hyperfine splitting for $\delta = 0$, given by $h\nu = 3A_\parallel/2$. As the microwave quantum is reduced towards this value a derivative minimum moves towards zero field, and below this value it is replaced by a derivative maximum. Measurements at several different frequencies indicate a value for $A_\parallel = 0.209 \pm 0.001$ $cm^{-1}$, which compares with $0.203 \pm 0.006$ $cm^{-1}$ from the high-field parameters.

## 5. Discussion

It is clear from the ratios $A_\parallel/g_\parallel\mu_B$ that these EPR spectra are indeed due to $Tm^{3+}$ and $Tb^{3+}$ ions. As the Zeeman interaction and magnetic hyperfine interaction are both linear in $J$, they project in the same way from the $J$ subspace to that of the effective spin $s$, assuming that small effects from matrix elements between different $J$ manifolds can be

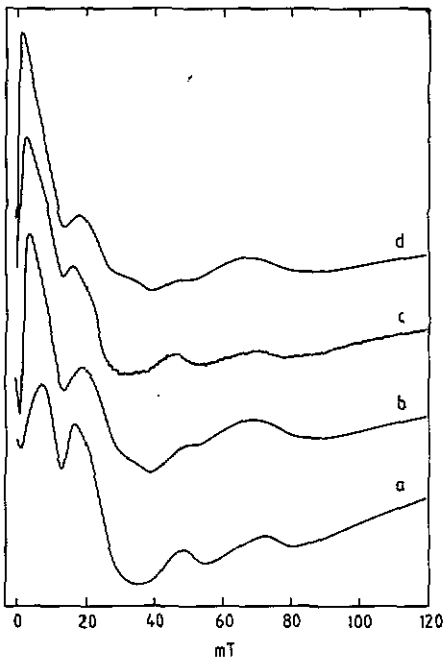


**Figure 3.** The EPR spectra of $Tb^{3+}$: (*a*) experimental spectrum at 9.50 GHz; (*b*) theoretical reconstruction for 9.50 GHz with $P(\delta) \propto \delta$; (*c*) experimental spectrum at 9.10 GHz; (*d*) theoretical reconstruction for 9.10 GHz with $P(\delta) \propto \delta$. The minimum seen at low field in (*a*) and (*b*) moves to zero field when $h\nu = 3A_\parallel/2$.

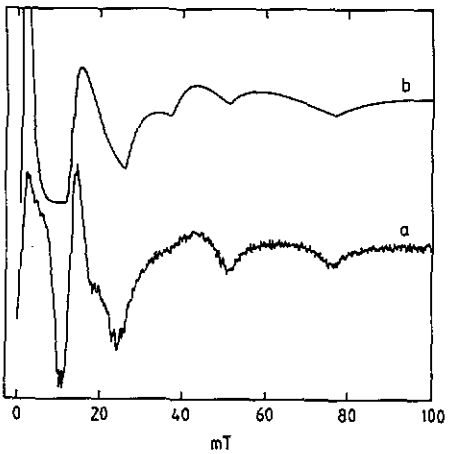


**Figure 4.** Second derivative of the $Tb^{3+}$ EPR spectra at 9.50 GHz: (*a*) experimental; (*b*) theoretical reconstruction with $P(\delta) \propto \delta$.

neglected. It follows that $A_\parallel$ and $g_\parallel$ are connected by the relation $A_\parallel/g_\parallel = A_J/g_J$, where the hyperfine interaction is taken to be $A_J \boldsymbol{J} \cdot \boldsymbol{I}$ and $g_J$ is the Landé factor. This ratio is independent of the nature of the ground state as modified by the local crystal field. The values measured directly in the present work agree well with those reported for these ions in a variety of crystalline materials. For $Tm^{3+}$ [5–9] reported values for $A_\parallel/g_\parallel\mu_B$ are all between 23.9 and 24.4 mT, compared to our value of 24.5 ± 1.0 mT. For $Tb^{3+}$ [4, 6, 10–13] $A_\parallel/g_\parallel\mu_B$ values range between 24.7 and 25.5 mT compared to our values of 24.9 ± 0.4 mT. Unfortunately this ratio alone gives no information at all about the geometry of the lanthanide ion sites.

Measurements of $A_\parallel$ or $g_\parallel$ individually can provide information about the sites. The crystal-field Hamiltonian for a lanthanide ion can be written:

$$\mathcal{H} = \langle J\|\alpha\|J\rangle \sum_q C_2^q O_2^q + \langle J\|\beta\|J\rangle \sum_q C_4^q O_4^q + \langle J\|\gamma\|J\rangle \sum_q C_6^q O_6^q$$

where $O_k^q$ ($q = 0, \ldots, k$) are angular momentum operators and $\langle J\|\alpha\|J\rangle$, $\langle J\|\beta\|J\rangle$ and $\langle J\|\gamma\|J\rangle$ are Stevens coefficients. The $C_k^q$ parameters are related to the $A_k^q$ defined in [4] by

$$C_k^q = A_k^q \langle r^k \rangle.$$

The $q = 0$ terms have axial symmetry about the $z$ axis. With only these terms the $J = 6$

manifolds of $Tm^{3+}$ and $Tb^{3+}$ would split into six doublets characterized by $|M_J\rangle = |\pm 6\rangle$, $|\pm 5\rangle$, $|\pm 4\rangle$, $|\pm 3\rangle$, $|\pm 2\rangle$, $|\pm 1\rangle$ and a singlet $|0\rangle$. The $q > 0$ terms have lower symmetry and mix states whose $M_J$ values differ by $\pm q$ and can split the doublets. For sites of fairly high symmetry some doublets may remain; for example, in sites with fourfold rotational symmetry the $C_4^4$ and $C_6^4$ terms will give three doublets from $|\pm 5\rangle$, $|\pm 1\rangle$, $|\mp 3\rangle$ but singlets from $|\pm 6\rangle$, $|\pm 2\rangle$ and from $|\pm 4\rangle$, $|\pm 0\rangle$. But generally, for low-symmetry sites, singlet levels are expected. The present EPR results show not only that, for an appreciable number of $Tm^{3+}$ and $Tb^{3+}$ ions, the ground states are closely spaced doublets, but also that since their $g_\parallel$ values are very close to $12g_J$, the states must be predominantly $|M_J\rangle = |\pm 6\rangle$. This shows that, with a suitable choice of coordinate axes, the crystal-field interaction is dominated by terms with axial symmetry, $C_2^0$, $C_4^0$ and $C_6^0$. It is difficult to estimate the proportion of ions in this state. Although the number contributing to the observed EPR signals could in principle be determined from the doubly integrated intensity of the measured spectra, the effect of a small uncertainty in the baseline at high fields introduces enormous errors, so this is not a useful procedure. But the signal seems to be stronger than would be expected for a totally random crystal field and indicates that certain geometrical arrangements of fluorines around each lanthanide ion are favoured.

Trivalent lanthanide ions in fluoride glasses are expected to have coordination numbers between 8 and 9 [14], with eightfold coordination becoming increasingly preferred in the second half of the series as the ionic radii decrease with increasing atomic number. Related crystal structures display a variety of lanthanide sites, many with low symmetry. Although a diversity of sites is likely in the glass, our results suggest at least a tendency for the ions to impose some local order, adopting sites that are relatively well defined and of high symmetry. We have therefore considered some of the possible arrangements (figure 5) of eight or nine fluorine ligands around a central lanthanide ion to see what sort of ground states might be expected. In these arrangements we have taken all the Ln–F separations $R_L$ to be equal. Neglecting any angular dependence of the bond energies, the most favoured structure should then be that which maximizes the separations of neighbouring fluorines. For eightfold coordination the square (Archimedean) antiprism with $D_{4d}$ symmetry is the arrangement that achieves this. The tetragonal dodecahedron with $D_{2d}$ symmetry is very nearly as good in this respect. Similar considerations for ninefold coordination indicates that the tricapped trigonal prism with $D_{3h}$ symmetry should be the most favoured arrangement followed by the monocapped square antiprism with $C_{4v}$ symmetry. All these arrangements have a clear principal symmetry axis, a feature that is necessary to understand the EPR.

The problem of estimating the crystal-field parameters $C_k^q$ for the site geometry is not simple, as the mechanism whereby a paramagnetic ion interacts with its immediate neighbours involves both electrostatic and chemical effects. An approach that has proved particularly useful for rare-earth ions has been the 'superposition model' [15], in which the contribution from each neighbouring ligand is taken to be axially symmetric about the line from its centre to the paramagnetic ion. These contributions are then summed over just the nearer neighbours. The size of each contribution is assumed to depend only on the type of ligand and its distance from the paramagnetic ion and is determined empirically from experimental results on known structures. One result of these calculations is that the terms of rank $k = 2$ are usually greater than those with $k = 4$, which in turn are greater than those with $k = 6$. This raises an immediate problem in interpreting the present results because the factor $\langle J\|\alpha\|J\rangle$ is of opposite sign for $Tb^{3+}$

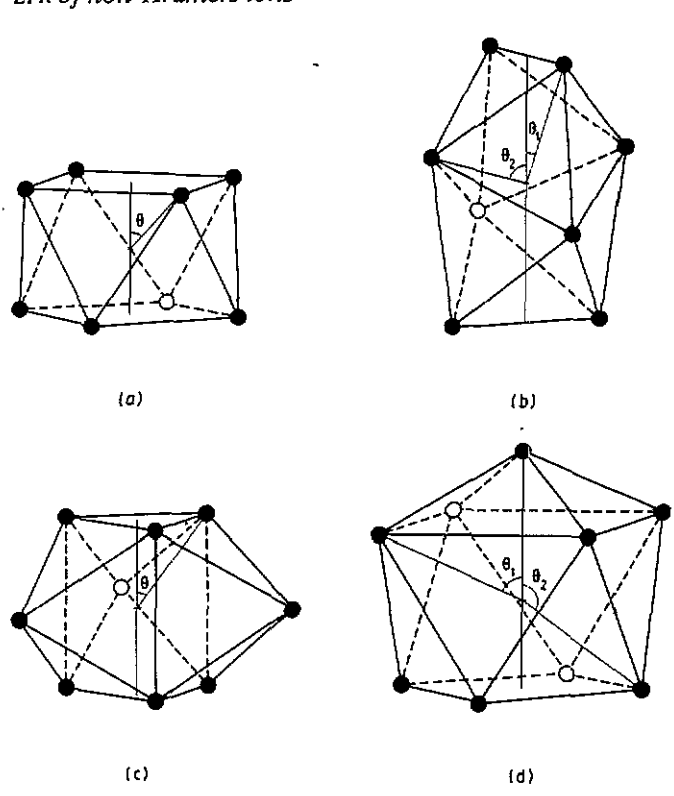


**Figure 5.** Possible fluorine coordinations around a lanthanide site. Ln–F separations are assumed equal and the angles shown were chosen to maximize F–F separations. (*a*) Square antiprism, with $\theta = 59.3°$ (Archimedean) or $\theta = 54.7°$ (cubic). (*b*) Tetragonal dodecahedron, with $\theta_1 = 36.8°$ and $\theta_2 = 69.5°$. (*c*) Tricapped trigonal prism, with $\theta = 41.8°$. (*d*) Monocapped square antiprism, with $\theta_1 = 70.1°$ and $\theta_2 = 125.7°$.

and $Tm^{3+}$. If both ions occupy a similar unique site, it must be one in which the contributions to $C_2^0$ tend to cancel to zero to produce $|\pm 6\rangle$ ground states for both ions. A more likely alternative is that the EPR is due to the two ions in different kinds of site.

Using the superposition model the crystal-field parameters are given by

$$C_k^q = \sum_L \bar{A}_k K_{kq}(\theta_L, \varphi_L)$$

where the coordination factors $K_{kq}(\theta_L, \varphi_L)$ are related to spherical harmonics and listed in [15]. The intrinsic parameters $\bar{A}_k$ are functions of the ligand distance $R_L$, but as we are taking $R_L$ to be the same for all ligands, they are taken to be constants. We have used the values below suggested by Yeung and Newman [16] from their analysis of $Er^{3+}:LaF_3$. These values are believed to be reasonably representative for any lanthanide ion at its standard lanthanide–fluorine spacing, and in any case a small variation in any of them will not critically affect our conclusions:

$$\bar{A}_2 = 240\ \text{cm}^{-1} \qquad \bar{A}_4 = 74\ \text{cm}^{-1} \qquad \bar{A}_6 = 19.4\ \text{cm}^{-1}.$$

The crystal-field parameters determined by this method are listed in table 2 and from

**Table 2.** Crystal-field parameters ($cm^{-1}$) for the coordination polyhedra of figure 5, calculated using superposition theory.

| | Tetragonal dodecahedron | Square antiprism (Archimedean) | Square antiprism (cubic) | Trigonal capped prism | Monocapped square antiprism |
|---|---|---|---|---|---|
| $C_2^0$ | 139.4 | −207.7 | 0.0 | 120.0 | −62.0 |
| $C_4^0$ | −74.8 | −181.2 | −230.2 | −75.7 | −43.4 |
| $C_4^4$ | 1163.2 | 0.0 | 0.0 | 0.0 | 448.9 |
| $C_6^0$ | −13.0 | 49.0 | 34.5 | −49.3 | 51.6 |
| $C_6^4$ | 322.0 | 0.0 | 0.0 | 0.0 | −298.7 |
| $C_6^6$ | 0.0 | 0.0 | 0.0 | 493.9 | 0.0 |

**Table 3.** Energy levels ($cm^{-1}$) for $Tm^{3+}$ and $Tb^{3+}$ in the coordination polyhedra of figure 5, calculated using the parameters of table 2.

| Tetragonal dodecahedron | Square antiprism (Archimedean) | Square antiprism (cubic) | Trigonal capped prism | Monocapped square antiprism |
|---|---|---|---|---|
| *Thulium* | | | | |
| 177.9 | | | | |
| 171.9 | 162.1 × 2 | 229.2 × 2 | 195.5 | 182.4 × 2 |
| 171.4 × 2 | 141.1 × 2 | 204.8 × 2 | 138.0 × 2 | 136.5 |
| 83.2 | 38.0 × 2 | 58.9 × 2 | 59.7 | 21.1 |
| 63.5 × 2 | 22.1 | 57.0 × 2 | 52.6 | 19.5 |
| 33.6 | 9.8 × 2 | −115.5 × 2 | 28.0 | 4.7 |
| 30.7 | −2.3 × 2 | −130.9 | −2.1 × 2 | −5.1 × 2 |
| −231.5 | −359.8 × 2 | −255.4 × 2 | −41.3 × 2 | −38.8 |
| −241.1 × 2 | | | −160.4 × 2 | 70.4 × 2 |
| −253.2 | | | −204.0 | −175.7 |
| | | | | −181.1 |
| *Terbium* | | | | |
| 171.1 | 179.9 × 2 | 160.0 × 2 | 82.9 | 79.5 × 2 |
| 166.9 × 2 | 137.0 × 2 | 127.7 × 2 | 60.5 × 2 | 61.8 |
| 161.0 | 22.5 × 2 | 78.7 × 2 | 49.4 | 30.8 |
| 45.2 | −2.4 × 2 | −25.0 × 2 | 28.4 × 2 | 29.4 |
| −1.8 × 2 | −86.7 × 2 | −102.4 × 2 | 7.2 × 2 | 9.7 |
| −82.3 | −158.7 × 2 | −130.4 | −11.9 | 8.9 × 2 |
| −107.3 | −183.3 | −173.9 × 2 | −30.1 × 2 | −25.1 |
| −108.3 × 2 | | | −125.9 | −66.5 |
| −146.8 | | | −126.5 | −69.7 × 2 |
| −154.5 | | | | −77.5 |

these we have calculated the energy levels and states. The energy levels are listed in table 3.

For the dodecahedron the ground states are singlets for both $Tm^{3+}$ and $Tb^{3+}$. The $|\pm 6\rangle$ states are not low-lying and are strongly mixed and well split by the large $C_4^4$ and $C_6^4$ terms. For $Tm^{3+}$ there is a doublet state only 12 $cm^{-1}$ above the ground state but all

components of its calculated $g$-tensor are small. It is clear that a $|\pm 6\rangle$ doublet ground state could not be produced for either ion by minor variations of the ligand positions and that this type of site is not responsible for the observed EPR.

The square antiprism is the only configuration that we are considering that has effectively pure axial symmetry and hence pure $|M_J\rangle$ states. For an Archimedean antiprism (with $\theta = 59.3°$ in figure 5($a$) and equilateral triangular faces) a $|\pm 6\rangle$ ground doublet is predicted for $Tm^{3+}$. As it is well separated from all the other levels, slight variations in site geometry will lead to only small splittings of this doublet. We therefore consider it highly probable that such sites account for the present $Tm^{3+}$ EPR. We note that a site with similar symmetry was proposed by Kazanskii [9] in interpreting the optically detected EPR of $Tm^{3+}$ in fluorite crystals, where $g_{\|} = 14$ was measured and related to ions within lanthanide clusters of the type $Y_6F_{37}$. A square antiprism is also closely related to the bicapped trigonal prismatic geometry occurring in the $YF_3$ structure, which is adopted in all the lanthanide trifluorides from samarium to lutetium. For $Tb^{3+}$ in the Archimedean antiprism, the dominant contribution to the energies from the $C_2^0$ term is of opposite sign and the predicted ground state is the $|0\rangle$ singlet. However, parameters are sensitive to changes of geometry, and a small modification to this arrangement that increases the negative charge density near the axis of the antiprism could lead to a $|\pm 6\rangle$ doublet ground state for this ion also. For example, the addition of two more distant fluorine neighbours to form a bicapped square antiprism could have this effect, as could an axial extension of the configuration that reduces $\theta$. To illustrate this we show in table 3 the levels for a square antiprism with $\theta = 54.7°$. (We refer to this as a 'cubic' antiprism, as it corresponds to a cube with one face rotated through 45° in its own plane. It has the property that $K_{20}$ and hence $C_2^0$ are zero.) Thus if the arrangement of fluorine ligands around a lanthanide ion is a square antiprism, it must be modified in one of these ways to account for the $Tb^{3+}$ EPR. It is interesting to note the EPR results reported for $Tm^{3+}$ [8] and $Tb^{3+}$ [13] in lanthanide nicotinate dihydrates, where both ions were also found to have nearly degenerate doublet ground states with $|M_J\rangle = |\pm 6\rangle$. Although the sites have very low symmetry in these crystals, the surrounding oxygens lie at the vertices of a rather distorted square antiprism.

Turning to possible 9-coordinated sites, the calculated ground state for $Tb^{3+}$ in a tricapped trigonal prism site consists of two closely spaced singlets with a small splitting $\delta \simeq 0.6\ cm^{-1}$. The states are essentially $|\pm 6\rangle$ and the splitting is associated with a small admixture of $|0\rangle$ introduced by the $C_6^6$ term. Variations in ligand position would give rise to a distribution of $\delta$ values, so sites of this type could clearly give rise to the observed EPR. Such sites are occupied by all lanthanide ions from lanthanum to thulium in the $NaLnF_4$ crystal structure, so it is highly probable that some occur in the glass and give rise to the $Tb^{3+}$ EPR. However, for $Tm^{3+}$ in this site, the predicted ground state is a singlet well separated from other states. The other common 9-coordinated site, the monocapped square antiprism, would have singlet ground states for both ions. This arrangement would have to be considerably distorted to produce a doublet capable of giving the observed EPR.

## 6. Conclusions

We have shown how EPR spectra of the two non-Kramers lanthanide ions $Tm^{3+}$ and $Tb^{3+}$ in a fluorozirconate glass have been interpreted by assuming closely spaced electronic doublet ground states with a range of values for the zero-field splitting parameter $\delta$. The

$g_{\|}$ values show that a substantial number of both ions have essentially a $|\pm 6\rangle$ ground state, indicating that the sites contributing to the EPR are relatively well defined but with a continuous range of small variations from site to site. It is unlikely that these results could arise from a random arrangement of fluorines around each lanthanide, and this indicates that certain characteristic arrangements are preferred. The $Tm^{3+}$ results are probably due to ions occupying 8-coordinated square antiprism sites, and the results for $Tb^{3+}$ are consistent with ions in a 9-coordinated tricapped trigonal prism site. Other structures could also occur, it is unfortunate that the numbers of ions in these sites cannot be determined experimentally from the EPR. However, the tendency, suggested by the present results, to progress from nine- to eight-fold coordination on going from $Tb^{3+}$ to $Tm^{3+}$ would be consistent with the expected reduction in bond length.

## Acknowledgments

We are grateful to Dr J M Parker and Dr A J Smith for valuable discussions. One of us (DF) is indebted to SERC and British Telecom for a CASE studentship.

## References

[1] France P W, Carter S F, Day C R and Moore M W 1989 *Fluoride Glasses (Critical Reports on Applied Chemistry 27)* ed A E Comyns (Chichester: Wiley) pp 87–122
[2] Griscom D L 1980 *J. Non-Cryst. Solids* **40** 211–72
[3] Harris E A and Furniss D 1988 *J. Phys. C: Solid State Phys.* **21** 7–15
[4] Abrgam A and Bleaney B 1970 *Electron Paramagnetic Resonance of Transition Ions* (Oxford: Clarendon)
[5] Gruber J B, Karlow E A, Olsen D N and Ranon U 1970 *Phys. Rev.* B **2** 49–53
[6] Schwab G and Hillmer W 1975 *Phys. Status Solidi* b **70** 237–44
[7] Yu J T 1976 *J. Phys. Chem. Solids* **37** 301–3
[8] Baker J M, Hutchison C A and Martineau P M 1986 *Proc. R. Soc.* A **403** 221–33
[9] Kazanskii S A 1985 *Zh. Eksp. Teor. Fiz.* **89** 1258–68 (Engl. Transl. 1985 *Sov. Phys.–JETP* **62** 727–33)
[10] Berulava B G and Sanadze T I 1960 *Paramagnetic Resonance* (Kazan: Kazan State University) p 11
[11] Forrester P A and Hempstead C F 1962 *Phys. Rev.* **126** 923–9
[12] Hutchison C A and Wong E 1958 *J. Chem. Phys.* **29** 754
[13] Baker J M, Hutchison C A, Leask M J M, Martineau P M, Robinson M G and Wells M R 1987 *Proc. R. Soc.* A **413** 515–28
[14] Poulain M 1989 *Fluoride Glasses (Critical Reports on Applied Chemistry 27)* ed A E Comyns (Chichester: Wiley) pp 11–48
[15] Newman D J and Ng B 1989 *Rep. Prog. Phys.* **52** 699–763
[16] Yeung Y Y and Newman D J 1985 *J. Chem. Phys.* **82** 3747–52